ISSN 1063-7710, Acoustical Physics, 2010, Vol. 56, No. 6, pp. 831–839. © Pleiades Publishing, Ltd., 2010.

Multifield Modeling of Cosserat Lattice Dynamics

A. A. Vasiliev

Tver' State University, per. Sadovyi 35, Tver', 170002 Russia

e-mail: alvasiliev@yandex.ru

Received March 1, 2010

Abstract—A two-field and a version of a four-field micropolar modes of a medium with a microstructure are constructed. A structural model of the Cosserat lattice taking into account both translational and rotational degrees of freedom of the medium elements and corresponding waves is used as a basic one. The models are constructed based on a one-dimensional doubling of the unit cell and a corresponding increase in the number of fields for deformation description. Based on comparison with a discrete, single-field, and four-field micropolar models, it is shown that a multifield approach makes it possible to construct a system of models that describe dynamics of the bodies with a microstructure taking into account not only long-wave, but also short-wave, deformations.

DOI: 10.1134/S1063771010060060

INTRODUCTION

Models of the classical mechanics of continuum media have been sufficiently developed and are widely and successfully used for the solution of practical problems. A well-developed and verified system of interconnected continual theories of physics and mechanics has already been formed. Models of them, a mathematical apparatus, and numerical and analytical methods have been developed.

However, there are number of effects related to the structure that classical models do not describe or yield a substantial error for during description. Models of generalized mechanics are being developed to take them into account. A generalized theory began intensively developing in the 1950s–1960s, and the key results were summarized at the historical IUTAM Symposium on the generalized Cosserat continuum and the continuum theory of dislocations with applications and in the proceedings of this symposium [1]. The problems of classical continuum theories are solved in the generalized mechanics by correcting their basic hypotheses, models, and notions.

At present, the models of Cosserat bodies and the micropolar theory [2, 3] are well developed and are widely used for modeling of bodies the deformation description of which necessitates taking into account of rotations of their structural elements. Since the beginning of the 1990s, models of high-gradient mechanics which take into account higher gradient field as compared to the models of classical mechanics have begun actively being developed [4, 5]. However, the problem of developing a physical theory that takes into account short-wave deformations within the framework of the generalized continuum theory is still relevant. The present study gives the development of a multifield approach [6–10] within the framework of which this problem seems to find a solution.

Another challenging theory lies in developing complex models based on the ideas and approaches of different theories of the generalized mechanics for constructing adequate models describing with high accuracy the effects of the bodies with a microstructure which are of interest to us.

DISCRETE AND SINGLE-FIELD MICROPOLAR THEORY

Let us consider a square Cosserat lattice (Fig. 1a) whose kinematics should be described taking into account not only translational displacements u_n, v_n, but also rotations φ_n of its elements as a basic one. The interaction of the elements k and m is described using the potential [11]

$$E_{\text{pot}}^{k,m} = \frac{1}{2}K_n^{k,m}(u_m - u_k)^2 + \frac{1}{2}K_s^{k,m}\left(v_m - v_k - r_{k,m}\frac{\varphi_m + \varphi_k}{2}\right)^2 + \frac{1}{2}G_r^{k,m}(\varphi_m - \varphi_k)^2, \quad (1)$$

where $r_{k,m}$ characterizes the distance between the elements and the constants $K_n^{k,m}$, $K_s^{k,m}$, and $G_r^{k,m}$ determine resistance to relative longitudinal and transverse displacements and element rotations. A spring-type

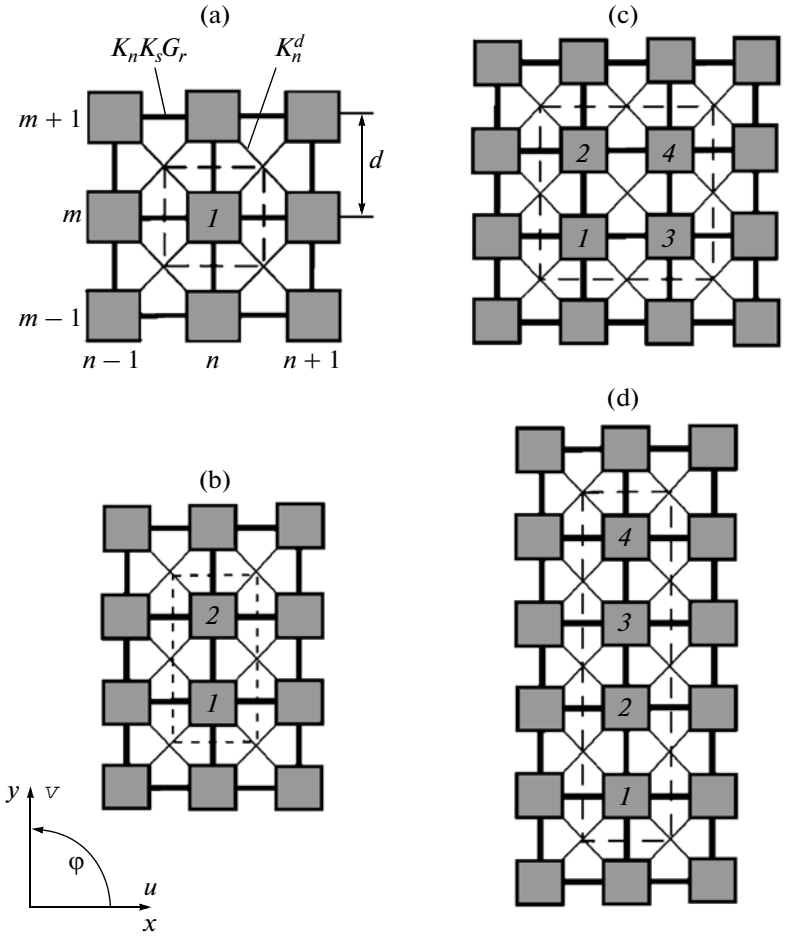

Fig. 1. A square Cosserat lattice (a), unit cell. Notation, macrocells from two and four particles (b)–(d).

model is used for diagonal connectives assuming that $K_s^d = G_r^d = 0$.

The potential energy of type (1) is a discrete analog of the potential energy accepted in the micropolar theory of elasticity [3]. It is used in discrete models of granulated media [11, 12] for modeling molecular crystals, material and constructions with beam-type connections which resist to rotation of the elements. Modeling of the crystal dynamics based of a microstructure lattice model taking into account the finite size and rotation of the particles with the potential which is an analog of the potential of type (1) [13] is considered in [14–16]. The microstructure parameters taken from the experimental data for a number of crystals based on a model with a square lattice were obtained in [15].

The kinetic energy of the kth element is taken in the form

$$E_{\text{kin}}^k = \frac{1}{2}M\dot{u}_k^2 + \frac{1}{2}M\dot{v}_k^2 + \frac{1}{2}J\dot{\varphi}_k^2.$$

The equations of motion of the element (n, m) are constructed based on the Lagrangian

$$\begin{aligned}
M\ddot{u}_{n,m} &= K_n\Delta_{xx}u_{n,m} + K_s\left(\Delta_{yy}u_{n,m} + \frac{1}{2}h\Delta_y\varphi_{n,m}\right) \\
&+ \frac{1}{2}K_n^d(\Delta u_{n,m} + \Delta_{xy}v_{n,m}), \\
M\ddot{v}_{n,m} &= K_n\Delta_{yy}v_{n,m} + K_s\left(\Delta_{xx}v_{n,m} - \frac{1}{2}h\Delta_x\varphi_{n,m}\right) \\
&+ \frac{1}{2}K_n^d(\Delta v_{n,m} + \Delta_{xy}u_{n,m}), \\
J\ddot{\varphi}_{n,m} &= \left(G_r - \frac{1}{4}K_sh^2\right)(\Delta_{xx}\varphi_{n,m} + \Delta_{yy}\varphi_{n,m}) \\
&+ \frac{1}{2}K_sh(\Delta_x v_{n,m} - \Delta_y u_{n,m} - 4h\varphi_{n,m}),
\end{aligned} \tag{2}$$

where the following notation is used

$$\Delta_x w_{n,m} = w_{n+1,m} - w_{n-1,m},$$

$$\Delta_{xx}w_{n,m} = w_{n+1,m} - 2w_{n,m} + w_{n-1,m},$$
$$\Delta_{y}w_{n,m} = w_{n,m+1} - w_{n,m-1},$$
$$\Delta_{yy}w_{n,m} = w_{n,m+1} - 2w_{n,m} + w_{n,m-1},$$
$$\Delta w_{n,m} = w_{n+1,m+1} + w_{n+1,m-1} - 4w_{n,m} + w_{n-1,m+1} + w_{n-1,m-1},$$
$$\Delta_{xy}w_{n,m} = w_{n+1,m+1} - w_{n+1,m-1} - w_{n-1,m+1} + w_{n-1,m-1}.$$

Expansion of displacements and rotations into the Taylor's series, with the derivatives not higher than the second order being taken into account, yields analogs of the equations of the micropolar elasticity theory,

$$\begin{aligned}
\rho U^{[1]}_{tt} &= (K_n + K_n^d)U^{[1]}_{xx} \\
&+ (K_s + K_n^d)U^{[1]}_{yy} + 2K_n^d V^{[1]}_{xy} + K_s\Phi^{[1]}_{y}, \\
\rho V^{[1]}_{tt} &= (K_s + K_n^d)V^{[1]}_{xx} \\
&+ (K_n + K_n^d)V^{[1]}_{yy} + 2K_n^d U^{[1]}_{xy} - K_s\Phi^{[1]}_{x}, \\
j\Phi^{[1]}_{tt} &= (G_r - K_s h^2/4)(\Phi^{[1]}_{xx} + \Phi^{[1]}_{yy}) \\
&+ K_s(V^{[1]}_{x} - U^{[1]}_{y} - 2\Phi^{[1]}),
\end{aligned} \tag{3}$$

where the denominations $\rho = M/h^2$ and $j = J/h^2$ are introduced and the index [1] is additionally used to note that only one vector field with the components $U^{[1]}(x, y, t)$, $V^{[1]}(x, y, t)$, and $\Phi^{[1]}(x, y, t)$ is used to describe medium deformation when constructing the continuum theory.

A TWO-FIELD MODEL AND A VERSION OF A FOUR-FIELD MODEL

Single-field model (3) was constructed based on dynamic equations (2) for a periodicity cell of a minimal size using one vector-function with the same degrees of freedom as those is a vector of generalized particle displacements. Note that there is a nonobvious assumption of a single-field theory. Rejection of this assumption leads to multifield models.

An N-field model is constructed based on a macrocell including N unit cells. An additional index $s = \overline{1, N}$ is introduced to mark the components of the vector of macrocell particle displacements $u^{[s]}_{n,m}(t)$, $v^{[s]}_{n,m}(t)$, and $\varphi^{[s]}_{n,m}(t)$. Then we write discrete equations of motion for the macrocell particles. The deformation of the system in the N-field model is described with N vector-functions with the components $u^{[s]}(x, y, t)$, $v^{[s]}(x, y, t)$, and $\varphi^{[s]}(x, y, t)$, $s = \overline{1, N}$. Now we construct $3N$ equations of motion of the N-field model with the help of expansion into the Taylor's series taking into account derivatives not higher than those of the second order.

A two-field model is constructed based on a macrocell including two unit cells (Fig. 1b). When new functions $U^{[1]} = (u^{[2]} + u^{[1]})/2$, $U^{[2]} = (u^{[2]} - u^{[1]})/2$, and analogous functions $V^{[s]}$, $\Phi^{[s]}$, $s = 1,2$ are introduced, the six connected equations split into two unconnected sets. The first set is a set of micropolar theory equations (3). The second set has the form

$$\begin{aligned}
MU^{[2]}_{tt} &= K_n h^2 U^{[2]}_{xx} - K_s[h^2(U^{[2]}_{yy} + \Phi^{[2]}_{y}) + 4U^{[2]}] \\
&- K_n^d[h^2(U^{[2]}_{xx} + U^{[2]}_{yy} + 2V^{[2]}_{xy}) + 4U^{[2]}], \\
MV^{[2]}_{tt} &= -K_n(h^2 V^{[2]}_{yy} + 4V^{[2]}) + K_s h^2(V^{[2]}_{xx} - \Phi^{[2]}_{x}) \\
&- K_n^d[h^2(V^{[2]}_{xx} + V^{[2]}_{yy} + 2U^{[2]}_{xy}) + 4V^{[2]}], \\
J\Phi^{(2)}_{tt} &= G_r[h^2(\Phi^{[2]}_{xx} - \Phi^{[2]}_{yy}) - 4\Phi^{[2]}] \\
&+ K_s h^2\left[\frac{1}{4}h^2(-\Phi^{[2]}_{xx} + \Phi^{[2]}_{yy}) + V^{[2]}_{x} + U^{[2]}_{y} - \Phi^{[2]}\right].
\end{aligned} \tag{4}$$

The authors of [17] used a macrocell with four particles shown in Fig. 1c to construct a four-field model. In the present work, we consider the macrocell shown in Fig. 1d. By introducing new field functions

$$U^{[1]} = \frac{1}{4}(u^{[4]} + u^{[3]} + u^{[2]} + u^{[1]}),$$
$$U^{[3]} = \frac{1}{4}(u^{[3]} - u^{[1]}),$$
$$U^{[2]} = \frac{1}{4}(u^{[4]} - u^{[3]} + u^{[2]} - u^{[1]}),$$
$$U^{[4]} = \frac{1}{4}(u^{[4]} - u^{[2]})$$

and analogous functions $V^{[s]}$, $\Phi^{[s]}$, $s = \overline{1,4}$ the set of 12 equations of a four-field models splits into three equations of a single-field micropolar theory (3), three auxiliary equations (4) of a two-field model, and a connected set of six equations

$$\begin{aligned}
MU^{[3]}_{tt} &= K_n h^2 U^{[4]}_{xx} \\
&+ K_s\left[\frac{1}{2}h^3\Phi^{[3]}_{yy} + h(2U^{[3]}_{y} + \Phi^{[3]}) - 2U^{[4]}\right] \\
&+ 2K_n^d[h(U^{[3]}_{y} + V^{[3]}_{x}) - U^{[4]}], \\
MV^{[3]}_{tt} &= 2K_n(hV^{[3]}_{y} - V^{[4]}) + K_s h^2(V^{[4]}_{xx} - \Phi^{[4]}_{x}) \\
&+ 2K_n^d[h(U^{[3]}_{x} + V^{[3]}_{y}) - V^{[4]}], \\
J\Phi^{[3]}_{tt} &= G_r(h^2\Phi^{[4]}_{xx} + 2h\Phi^{[3]}_{y} - 2\Phi^{[4]})
\end{aligned} \tag{5}$$

$$+ K_s h\Big[- U^{[3]} + h\Big(V_x^{[4]} - \frac{3}{2}\Phi^{[4]}\Big)$$

$$- \frac{1}{2}h^2(U_{yy}^{[3]} + \Phi_y^{[3]}) - \frac{1}{4}h^3\Phi_{xx}^{[4]}\Big],$$

and

$$MU_{tt}^{[4]} = K_n h^2 U_{xx}^{[3]}$$

$$+ K_s\Big[-\frac{1}{2}h^3\Phi_{yy}^{[4]} + h(-2U_y^{[4]} - \Phi^{[4]}) - 2U^{[3]}\Big]$$

$$+ 2K_n^d[- U^{[3]} - h(U_y^{[4]} + V_x^{[4]})],$$

$$MV_{tt}^{[4]} = 2K_n(-hV_y^{[4]} - V^{[3]}) + K_s h^2(V_{xx}^{[3]} - \Phi_x^{[3]})$$

$$+ 2K_n^d[-h(U_x^{[4]} + V_y^{[4]}) - V^{[3]}], \quad (6)$$

$$J\Phi_{tt}^{[4]} = G_r(h^2\Phi_{xx}^{[3]} - 2h\Phi_y^{[4]} - 2\Phi^{[3]})$$

$$+ K_s h\Big[U^{[4]} + h\Big(V_x^{[3]} - \frac{3}{2}\Phi^{[3]}\Big)$$

$$+ \frac{1}{2}h^2(U_{yy}^{[4]} + \Phi_y^{[4]}) - \frac{1}{4}h^3\Phi_{xx}^{[3]}\Big].$$

A COMPARATIVE ANALYSIS OF MODELS

A comparative analysis of models will be performed by construction and comparing dynamic solutions of the form

$$w_{k,m}(t) = \overline{W}e^{i(\omega t - kK_x - mK_y)}, \quad (7)$$

where $w_{k,m}(t)$ and $\overline{W}$ are the vectors with the components $u_{k,m}(t)$, $v_{k,m}(t)$, $\varphi_{k,m}(t)$ and $\overline{U}$, $\overline{V}$, $\overline{\Phi}$, respectively; $K_x = k_x h$, $K_y = k_y h$; k_x, k_y are the wave numbers; and ω is the frequency.

Substitution of Eqs. (7) into dynamics equations (2) yields a set of homogeneous algebraic equations

$$(a_{11} + M\omega^2)\overline{U} + a_{12}\overline{V} + a_{13}i\overline{\Phi} = 0,$$

$$a_{12}\overline{U} + (a_{22} + M\omega^2)\overline{V} + a_{23}i\overline{\Phi} = 0, \quad (8)$$

$$a_{13}\overline{U} + a_{23}\overline{V} + (a_{33} + J\omega^2)i\overline{\Phi} = 0,$$

with the components

$$a_{11} = 2(\cos K_x - 1)K_n + 2(\cos K_y - 1)K_s$$

$$+ 2(\cos K_x \cos K_y - 1)K_n^d,$$

$$a_{12} = -2K_n^d \sin K_x \sin K_y,$$

$$a_{13} = -hK_s \sin K_y, \quad (9)$$

$$a_{22} = a_{11}(x \leftrightarrow y), \quad a_{23} = hK_s \sin K_x,$$

$$a_{33} = -(\cos K_x + \cos K_y + 2)h^2 K_s/2$$

$$+ 2(\cos K_x + \cos K_y - 2)G_r.$$

The condition at which nontrivial solutions exist is a zero determinant of set (8). It yields dispersion equations which determine three dispersion surfaces $\omega = \omega(K_x, K_y)$ which are considered in the range of $0 \le K_x \le \pi$, $0 \le K_y \le \pi$.

The dispersion relations and the surfaces of continuum models are constructed for continuum analogs of solutions to Eq. (7) of the form

$$W^{[s]}(x, y, t) = \overline{W}^{[s]}e^{i(\omega t - k_x x - k_y y)}, \quad (10)$$

where $W^{[s]}(x, y, t)$ and $\overline{W}^{[s]}$ are the vectors with the components $U^{[s]}(x, y, t)$, $V^{[s]}(x, y, t)$, $\Phi^{[s]}(x, y, t)$, and $\overline{U}^{[s]}$, $\overline{V}^{[s]}$, $\overline{\Phi}^{[s]}$, respectively.

Substitution of Eq. (10) to equations of single-field micropolar model (3) yields a set of equations of type (8) where the matrix components are expansions of components (9) into the Taylor's series at the point $(K_x, K_y) = (0,0)$ taking into account the degrees not higher than those of the second order. Thus, three corresponding dispersion surfaces of a single-field micropolar model determined in the range of $0 \le K_x \le \pi$, $0 \le K_y \le \pi$ approximate dispersion surfaces of the discrete system at the point $(K_x, K_y) = (0,0)$ and, thus, there is a good agreement between discrete (2) and single-field (3) models in the range of long waves [11]. For short waves, a single-field micropolar model gives a substantial error and is inapplicable.

Substitution of the solution of type (10) into six equations of two-field model (3) and (4) gives six dispersion surfaces considered in the range of $0 \le K_x \le \pi$, $0 \le K_y \le \pi/2$. Three from the dispersion surfaces corresponding to single-field model equations (3) provides for approximation of the dispersion surfaces of the discrete system in the long-wave range. Using a comparative analysis it can be shown that the dispersion surfaces corresponding to auxiliary equation (4) of a two-field model determined in the range $0 \le K_x \le \pi$, $0 \le K_y \le \pi/2$ after reflection with respect to the plane $K_y = \pi/2$ to the region $0 \le K_x \le \pi$, $\pi/2 < K_y \le \pi$ approximate dispersion surfaces of the discrete system and short-wave ranges at the point $(K_x, K_y) = (0, \pi)$.

Four groups of the surfaces of a four-field model are determined in the range $0 \le K_x \le \pi$, $0 \le K_y \le \pi/4$. Three dispersion surfaces corresponding to single-field model equations (3) approximate the dispersion surfaces of the discrete system in the long-wave range. Three dispersion surfaces corresponding to Eqs. (4) after reflection with respect to the plane $K_y = \pi/2$ approximate the dispersion surfaces of the discrete model in the region $0 \le K_x \le \pi$, $3\pi/4 \le K_y \le \pi$ at the point $(K_x, K_y) = (0, \pi)$. Six dispersion surfaces corresponding to Eqs. (5) and (6) of a four-field model after reflection, and transfer approximate the dispersion

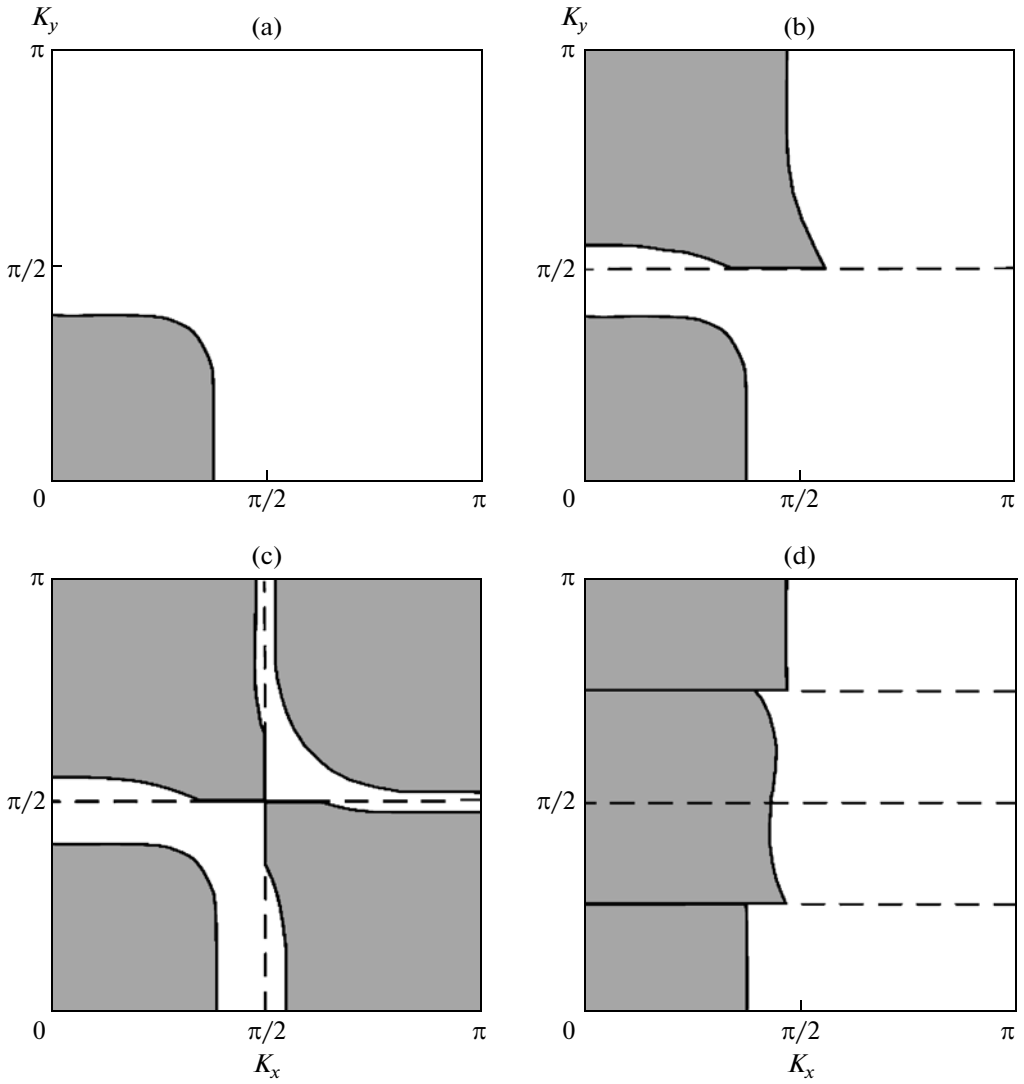

Fig. 2. The regions where the relative error of approximation of the dispersion surfaces of microrotations of a square Cosserat lattice by the dispersion surfaces of single-field (a), two-field (b), and four-field (c) models obtained in [17] (c) and in the present study (d) does not exceed 2.5%.

surfaces of the discrete model at the point $(K_x, K_y) = (0, \pi/2)$ in the ranges $0 \le K_x \le \pi$, $\pi/2 \le K_y < 3\pi/4$ and $0 \le K_x \le \pi$, $\pi/4 < K_y \le \pi/2$.

Figures 2 and 3 illustrate the performed analysis. Without losing community, one can fix, for example, K_n, M, and h. During the calculations the values of other parameters which are considered dependent are assumed to be $K_s = (1/3)K_n$, $G_r = (1/3)K_n h^2$, $K_n^d = 0.74K_n$, $J = (1/8)Mh^2$, which corresponds, e.g., to the case of a granulated media. Such parameters were used for the comparison of the dispersion curves of discrete (2) and single-field continuum (3) models in [11]. In [11], the comparison of continuum model equations (3) and phenomenological micropolar equations [3] yielded common correlations between the parameters of discrete (2) and micropolar models. Then, assuming that the constants of micropolar equations for a granulated media are known from a macroexperiment, the microstructure parameters are found.

Figure 2a shows the regions in the vicinity of the points $(K_x, K_y) = (0,0)$ where the relative error $|(\omega_{cont} - \omega_{discr})/\omega_{discr}|$ of the approximation of the wave surfaces of the discrete system microrotations $\omega_{discr}(K_x, K_y)$ by the corresponding dispersion surface $\omega_{cont}(K_x, K_y)$ of a single-field model does not exceed 2.5%. Figure 2b additionally shows the region in the vicinity of the point $(K_x, K_y) = (0, \pi)$ where such accuracy for the corresponding short waves is ensured by a two-field model. Figures 2c and 2d reflect distinctions of four-field models in [17] and those in the present paper. The model of [17] refines single-field micropolar model (3) during modeling waves and deformations

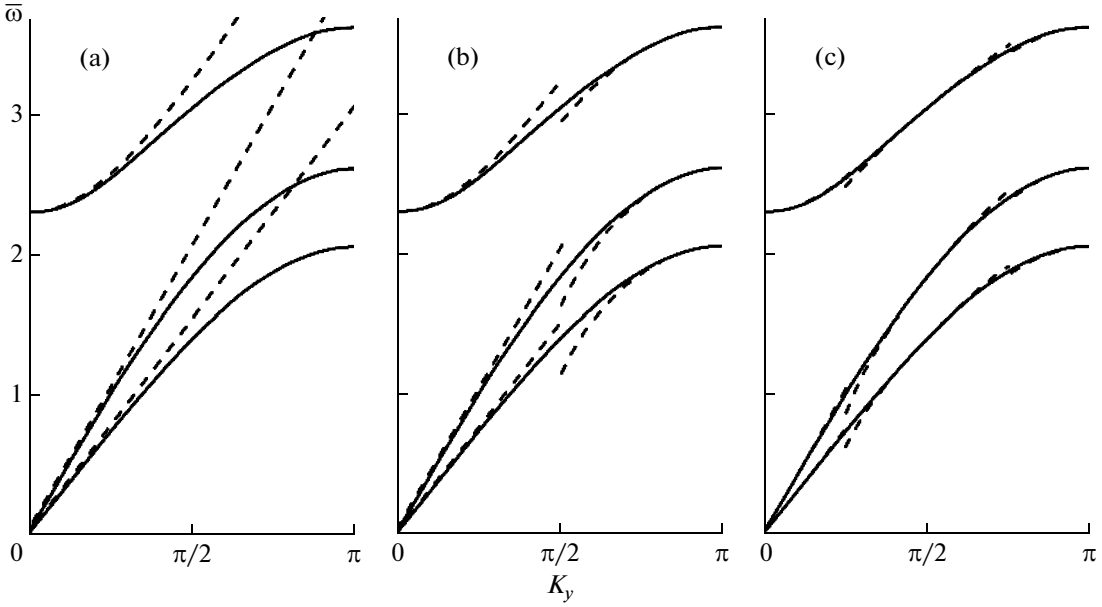

Fig. 3. Dispersion curves of a square Cosserat lattice in the section of dispersion surfaces by the plane $K_x = 0$ (solid lines) and their approximations by the dispersion curves of single-field (a), two-field (b), and four-field (c) models (dashed lines).

in highly-symmetric direction for the short waves with the wave numbers in the regions $(\pi, 0)$, $(0, \pi)$, and (π, π). Four-field model (3)–(6) gives refinement only for plane waves and deformations with $K_x = 0$. However, contrary to the model of [17], a micropolar model is refined only for the waves with the wavenumber not only near $(0, \pi)$, but also $(0, \pi/2)$. This refinement can be important when modeling thin interlayers and frequency filters.

A solid line in Fig. 3 shows dimensionless dispersion curves $\bar{\omega} = \omega\sqrt{M/K_n}$ in the cross section $K_x = 0$ of the dispersion surfaces of a discrete system, and dashed lines show their approximation by the dispersion curves of a single-field (a), a two-field (b), and a four-field (c) model. A single-field model provides a good accuracy of approximation of the dispersion curves of the discrete system in the long-wave range $K_y \approx 0$, however, its accuracy for short waves is substantial. The dispersion curves of a two-field model in the range of $0 \le K_y \le \pi/2$ coincide with the dispersion curves of a single-field model. A two-field model is accurate in the short-wave range for $K_y \approx \pi$. It is apparent in Fig. 3 that the maximal error of a two-field model is observed at the point $K_y = \pi/2$. A four-field model coincides with a two-field one at the intervals of $0 \le K_y \le \pi/4$, $3\pi/4 \le K_y \le \pi$ and refines it in the middle wavelengths for $K_y \approx \pi/2$.

ANALYSIS OF ONE-DIMENSIONAL DYNAMICS

A comparative analysis of the models taking into account those damped over the spatial variable can be performed for one-dimensional solution varying in highly symmetric directions. In the case of diagonal directions such analysis of the models is given in [13, 18]. Solutions and a corresponding analysis are of interest when studying edge effects in thin layers and constructing frequency filters and in nonlinear problems during a linear analysis of, e.g., discrete breathers.

The present work gives the analysis of constructing models for one-dimensional waves which do not change along the *OX* axis. The dispersion relations for this case obtained from Eqs. (8), (9) by substituting $K_x = 0$ split and, using denominations $\Omega = \omega^2$, $Z = 2(1 - \cos K_y)$ can be written as

$$M\Omega = (K_n + K_n^d)Z, \tag{11}$$

$$b_{11}Z^2 + 2b_{12}Z\Omega + b_{22}\Omega^2 + b_1 Z + b_2\Omega = 0, \tag{12}$$

where

$$b_{11} = (G_r - h^2K_n^d/4)K_s + G_rK_n^d, \quad b_{22} = MJ,$$

$$2b_{12} = -(G_r - h^2K_s/4)M - (K_s + K_n^d)J,$$

$$b_1 = (K_s + 2K_n^d)K_sh^2, \quad b_2 = -2MK_sh^2.$$

Let us consider the solution of type (7) which takes into account the solutions localized over the spatial variable assuming that $iK_y = K_{\mathrm{Re}} + iK_{\mathrm{Im}}$.

Straight line (11) intersects the straight line $Z = 4$ at $\Omega|_{Z=4} = 4(K_n + K_n^d)/M$. It determines the branch of harmonic solutions for the frequencies in the interval $0 \le \Omega \le \Omega|_{Z=4}$ and the branch of damped short-wave

solutions for the high frequencies $\Omega \geq \Omega|_{Z=4}$. From the condition $D = b_{11}b_{22} - b_{12}^2 > 0$, we obtain that curve (12) is elliptical in the region

$$\overline{JK}_n^d + \bar{J} - \sqrt{\bar{J}} + 1/4 < \bar{G}_r < \overline{JK}_n^d + \bar{J} + \sqrt{\bar{J}} + 1/4$$

of the dimensionless parameters $\bar{G}_r = G_r/K_s h^2$, $\bar{K}_n^d = K_n^d/K_s$, and $\bar{J} = J/Mh^2$ and hyperbolic beyond this region.

Curve (12) intersects the straight lines $Z = 0$ and $Z = 4$ at the points $\Omega|_{Z=0} = 0$, $\Omega|_{Z=0} = 2K_s h^2/J$ and $\Omega|_{Z=4} = 4(K_s + K_n^d)/M$, $\Omega|_{Z=4} = (4G_r + K_s h^2)/J$. The sections of curve (12) connecting these points in the interval $0 \leq Z \leq 4$ determine two branches of harmonic solutions. There is always sections of curve (12) determined in the range $Z \leq 0$ and $Z \geq 4$ which determine the branches of dispersion curves in the planes $K_{\mathrm{Im}} = 0$ and $K_{\mathrm{Im}} = \pi$ corresponding to monotonously varying solutions and short-wave localized ones. Note that the dispersion curves determined for $K_{\mathrm{Re}} \neq 0$, $K_{\mathrm{Im}} \neq 0$ correspond to the frequencies Ω for which there are no real values of Z. The structure medium is a filter for the waves in the regions where there are no harmonic solutions and only spatially localized solutions $K_{\mathrm{Re}} \neq 0$ are implemented. The boundaries of the frequency filter zone are determined by the values of the minima (maxima) of the dispersion curves of harmonic solutions which are reached either at the boundaries at the frequencies $\sqrt{\Omega}|_{Z=0}$, $\sqrt{\Omega}|_{Z=4}$ or inside the region $0 \leq K_{\mathrm{Im}} \leq \pi$.

In the problems of mechanics, the solutions in the range of low frequencies $\Omega \approx 0$ are of particular interest. The points of intersection with the axis $\Omega = 0$ determine static solutions. Curve (12) intersects the axis $\Omega = 0$ at the point $Z = 0$, which determines the linear part of a static solution. In case of positive parameter values, there are no points of intersection of the $\Omega = 0$ axis in the interval $0 < Z < 4$. This means that at such parameters the system is stable. The second point $Z|_{\Omega=0} = -b_1/b_{11}$ of the intersection of the axis $\Omega = 0$ is in the region $Z < 0$ or $Z > 4$. Monotonously decreasing effects are implemented in the systems of the first type, and short-wave edge effects are implemented in the systems of the second type. The parameter spaces of different types of systems are separated by the curve $\bar{G}_r = \bar{K}_n^d/4(1 + \bar{K}_n^d)$.

The analysis shows that single-field micropolar model (3) provides for a good approximation of the branches of harmonic and monotonously varying localized solutions of the discrete system in the planes $K_{\mathrm{Re}} = 0$ and $K_{\mathrm{Im}} = 0$ for the frequencies $\omega \approx \sqrt{\Omega|_{Z=0}}$ in the vicinity of the point $(K_{\mathrm{Im}}, K_{\mathrm{Re}}) = (0, 0)$. A single-field model describes monotonously damping ($K_{\mathrm{Im}} = 0$) static edge effects with weak localization ($K_{\mathrm{Re}} \approx 0$).

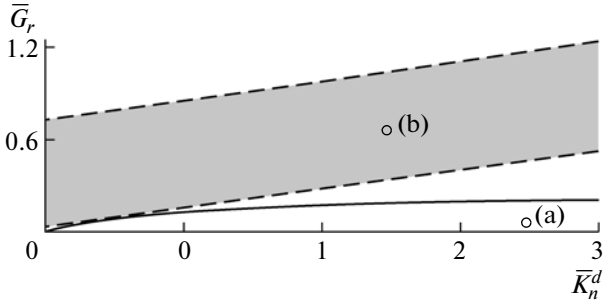

Fig. 4. The space of dimensionless parameters and the curves separating the regions with different types of dispersion curves and edge effects.

Only monotonously damping edge effects are implemented in a lattice with square cells without diagonal connections $\bar{K}_n^d = 0$. Note that as in [13] the systems where short-wave edge effects are realized can be constructed based on a structural model of the material with finite particle sizes [14–16, 19]. In this case a single-field micropolar model is inapplicable.

A two-field model contains Eqs. (3) of a single-field model and possesses its properties for long waves. Equations (4) of a two-field micropolar model provide for approximation of the branches of harmonic and short-wave localized solutions in the planes $K_{\mathrm{Re}} = 0$ and $K_{\mathrm{Im}} = \pi$ for the frequencies $\omega \approx \sqrt{\Omega}|_{Z=4}$ in the vicinity of the point $(K_{\mathrm{Im}}, K_{\mathrm{Re}}) = (\pi, 0)$. Thus, a two-field model gives exact values of $\sqrt{\Omega}|_{Z=0}$ and $\sqrt{\Omega}|_{Z=4}$ which determine the boundaries of the frequency filter zone of a discrete system in case the minimum (maximum) of the dispersion curves of harmonic solutions is reached at these values (Fig. 5b). If the minima (maxima) are in the interval $0 < K_{\mathrm{Im}} < \pi$ (Fig. 5a) four-field model (3)–(6) can be used to refine a two-field model in determining the frequency filter boundaries. In addition, a two-field model, contrary to a single-field one, reflects short-wave ($K_{\mathrm{Im}} = \pi$) static edge effects with weak localization ($K_{\mathrm{Re}} \approx 0$).

The performed analysis is demonstrated by Figs. 4 and 5. The space of dimensionless parameters $\bar{G}_r$, $\bar{K}_n^d$ to which curves (12) of an elliptical type for the lattices with $\bar{J} = 1/8$ correspond is shown in Fig. 4 by dashed lines. A solid line shows the curve which separates the parameters of the systems where monotonously varying and short-wave static edge effects determined by the points of intersection of the dispersion curves with the plane $\omega = 0$ (marked on the axes $\bar{\omega} = 0$ with circles) are implemented. Figures 5a and 5b represent the dispersion curves in the planes $K_{\mathrm{Im}} = 0$, $K_{\mathrm{Re}} = 0$, and $K_{\mathrm{Im}} = \pi$ constructed for a discrete system and approx-

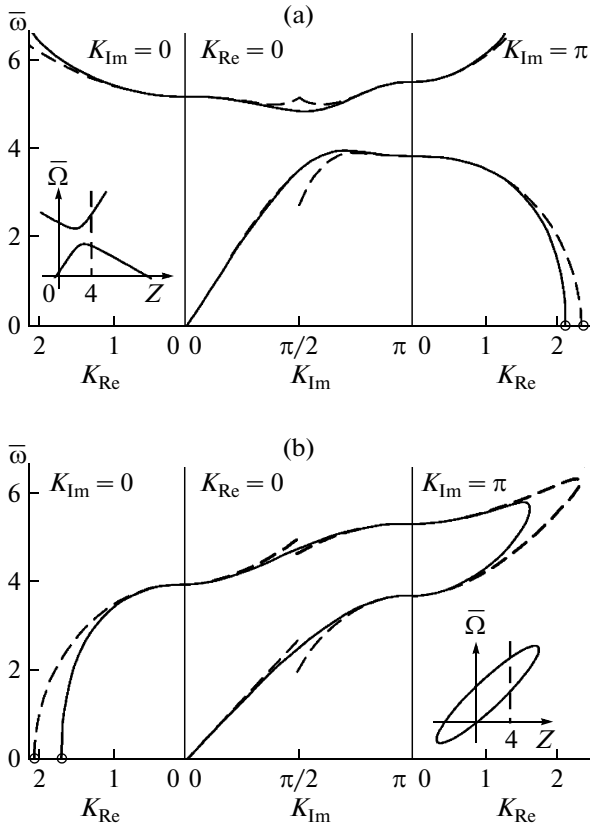

Fig. 5. Planes $K_{\mathrm{Im}} = 0$, $K_{\mathrm{Re}} = 0$, and $K_{\mathrm{Im}} = \pi$. The dispersion curves of a discrete system and their approximations by the curves of a two-field model (solid and dashed lines, respectively) constructed for the parameters marked with points (a) and (b) in Fig. 4.

imating their dispersion curves of a two-field model (solid and dashed lines, respectively). Two qualitatively different types of dispersion curves and edge effects for the dimensionless parameters $\bar{G}_r = 0.025$, $\bar{K}_n^d = 3.5$ and $\bar{G}_r = 0.65$, $\bar{K}_n^d = 2.5$. marked in Fig. 4 with the points (a) and (b) are exemplified.

CONCLUSIONS

The present work continues and develops studies [17–19] devoted to the development of the multifield theory of the Cosserat media.

The models were constructed based on the structural approach. This approach was effectively implemented when constructing dynamic theories in the solid state physics [20] and is useful for development and practical interpretation of phenomenological models. The Cosserat lattice where, contrary to classical lattices, rotations of structural elements are taken into account is used in the present study as a basic one.

A single-field version of model (3) constructed based on a unit cell is an analog of the equations of the micropolar elasticity theory. A high-gradient version of a single-field micropolar model which takes into account the fourth-order derivatives over spatial variables was constructed in [15, 18]. The development of the elasticity theory models of complex lattices taking into account momentary interactions at a microlevel is presented in [21]. The authors of [12] offer a nonlocal version of the Cosserat model where, contrary to a conventional micropolar model, the second derivatives of the rotation field are absent in the dynamic equation for rotations.

The system of the considered models of the Cosserat media illustrates the idea that there should be a system of models with different levels of complexity in the mechanics of media with a microstructure, which will make it possible to use during the investigations the most elementary and convenient models, which, however, adequately reflect the analyzed effects.

The problem of accounting in the model of short-wave effects based on clear physical assumptions is efficiently used in the multifield theory. Abstaining from an attempt to describe deformations of the system with one field based on a unit cell, introduction of macrocells into consideration, and an increase in the number of the fields used to describe system deformations allows constructing a hierarchic system of models which describe dynamics of a structural system with the required accuracy taking into account both long-wave and short-wave deformations.

In the present study, the models are constructed based on a combination of approaches of the micropolar and multifield theories that makes it possible to take into account rotational degrees of freedom of the medium elements and short-wave deformations. Note that the constructed continuum models do not describe a discrete system dispersion of one-dimensional waves in an elementary chain described by dispersion equation (11). It is possible to refine the model additionally applying the approaches of gradient mechanics taking into account the higher-order field derivatives. When modeling the lattices with complex cells that requires taking into account internal deformations of unit cells, it seems interesting to consider a combination of the approaches of the micromorph and multifield theories.

REFERENCES

1. *Mechanics of Generalised Continua: Proc. of the IUTAM Symp. on the Generalized Cosserat Continuum and the Continuum Theory of Dislocations with Applications, 1967*, Ed. by E. Kroner (Springer, Berlin, 1968).
2. E. Cosserat and F. Cosserat, *Theorie des Corps Deformables* (Hermann, Paris, 1909).
3. A. C. Eringen, in *Fracture, 2*, Ed. by H. Liebowitz (Academic, New York, 1968), p. 621.
4. E. C. Aifantis, Int. J. Eng. Sci. **30**, 1279 (1992).
5. N. Triantafyllidis and S. Bardenhagen, J. Elasticity **33**, 259 (1993).

6. E. A. Il'yushina, Prikl. Mat. Mekh. **33**, 917 (1969).
7. E. A. Il'yushina, Prikl. Mat. Mekh. **36**, 1086 (1972).
8. I. N. Molodtsov, Candidate's Dissertation in Mathematical Physics (Mosc. Gos. Univ., Moscow, 1982).
9. A. A. Vasil'ev, Candidate's Dissertation in Mathematical Physics (Tver. Gos. Univ., Tver, 1993).
10. A. A. Vasiliev, S. V. Dmitriev, and A. E. Miroshnichenko, Int. J. Solids Struct. **47**, 510 (2010).
11. A. S. J. Suiker, A. V. Metrikine, and R. de Borst, Int. J. Solids Struct. **38**, 1563 (2001).
12. E. Pasternak and H.-B. Muhlhaus, J. Eng. Math. **52**, 199 (2005).
13. A. A. Vasiliev, A. E. Miroshnichenko, and M. Ruzzene, Mech. Res. Commun. **37**, 225 (2010).
14. S. A. Lisina, A. I. Potapov, and V. F. Nesterenko, Akust. Zh. **47**, 666 (2001) [Acoust. Phys. **47**, 578 (2001)].
15. I. S. Pavlov, A. I. Potapov, and G. A. Maugin, Int. J. Solids Struct. **43**, 6194 (2006).
16. A. I. Potapov, I. S. Pavlov, and S. A. Lisina, J. Sound Vibrat. **322**, 564 (2009).
17. A. A. Vasiliev and A. E. Miroshnichenko, J. Mech. Behav. Mater. **16**, 379 (2005).
18. A. A. Vasiliev, A. E. Miroshnichenko, and M. Ruzzene, J. Mech. Mater. Struct. **3**, 1365 (2008).
19. A. A. Vasiliev, S. V. Dmitriev, and A. E. Miroshnichenko, Int. J. Solids Struct. **42**, 6245 (2005).
20. M. Born and K. Huang, *Dynamical Theory of Crystal Lattices* (Clarendon, Oxford, 1954; Inostr. Liter., Moscow, 1958).
21. E. A. Ivanova, A. M. Krivtsov, and N. F. Morozov, Prikl. Mat. Mekh. **71**, 595 (2007).
22. E. F. Grekova and G. C. Herman, in *Proc. of 66th EAGE (European Association of Geoscientists and Engineers) Conf.* (Paris, 2004), p. 98.
23. M. A. Kulesh, E. F. Grekova, and I. N. Shardakov, Akust. Zh. **55**, 216 (2009) [Acoust. Phys. **55**, 218 (2009)].